is dependent on the drawing tension [2]. The residual tensile stress in the core is expressed as [3]

$$\sigma = \frac{A_2 E_2 f}{(A_1 E_1 + A_2 E_2) A_1} \left(1 + \frac{\eta_2 A_2}{\eta_1 A_1}\right)^{-1} \quad (2)$$

where A is the cross-sectional area, E is the Young modulus, f is the drawing tension, η is the viscosity at the softening temperature, and the subscripts 1 and 2 represent the core and cladding, respectively.

If the optical loss change is due to the residual stress which arises during drawing, from eqn. 2, it is necessary to match the viscosities of the core and cladding to decrease the residual stress in the core. However, it is unclear at what temperature the viscosity difference between the core and cladding influences the optical property of the fibre. We are now considering matching the viscosity of the core and cladding over a relatively wide temperature range, such as from 1200 to 2200°C. As seen from Fig. 4, it is appropriate to match the viscosity of the core and cladding at a low temperature because the viscosity sensitivity $d[\log \eta]/d[F]$ is larger than that at a high temperature.

Therefore, to achieve ultralow-loss fibre, we should select fibre materials taking their viscosities into account as well as their Rayleigh scattering and infra-red absorption losses.

Conclusions: The viscosity of F-doped silica glass is investigated experimentally. The F concentration dependence of the viscosity in F-doped silica glasses is clarified. We found that the viscosity difference between pure silica and F-doped silica glasses becomes smaller as the temperature increases. This experimental result will be useful when fibre materials are designed for the fabrication of low-loss fibres.

Acknowledgments: The authors would like to thank H. Takahashi, S. Suzuki, and R. Yamauchi for fabricating the sample glasses. Thanks are also due to Y. Wakui, K. Ishihara, and M. Kawase for their continuous encouragement.

24th March 1992

M. Ohashi, M. Tateda, K. Tajima and K. Shiraki (*NTT Telecommunication Field Systems R&D Center, Tokai, Ibaraki-ken, 319-11 Japan*)

References

1 YOKOTA, H., KANAMORI, H., ISHIGURO, Y., TANAKA, G., TANAKA, S., TAKADA, H., WATANABE, M., SUZUKI, S., YANO, K., HISHIKAWA, M., and SHINBA, H.: 'Ultra-low-loss pure-silica-core single-mode fiber and transmission experiment'. Tech. Dig. on Optical Fiber Communication, postdeadline paper PDP3, 1986

2 HANAWA, B., HIBINO, Y., and HORIGUCHI, M.: 'Drawing condition dependences of pure-silica-core single-mode fibers', *Trans. IEICE, Japan*, 1989, **J72-C-I**, pp. 167–176

3 HIBINO, Y., EDAHIRO, T., HORIGUCHI, T., AZUMA, Y., and SHIBATA, N.: 'Evaluation of residual stress and viscosity in SiO_2-core/F-SiO_2 clad single-mode optical fibers from Brillouin gain spectra', *J. Appl. Phys.*, 1989, **66**, pp. 4049–4052

4 OHASHI, M., SHIRAKI, K., and TAJIMA, K.: 'Optical loss property of silica-based single-mode fibers', *J. Lightwave Technol.*, 1992, **LT-10**, (2)

5 DOUGLAS, R. W., ARMSTRONG, W. L., EDWARD, J. P., and HALL, D.: 'Penetration viscometer', *Glass Tech.*, 1975, **6**, pp. 52–55

6 OH, S. M.: 'Cooling rates of optical fibres during drawing', *Am. Ceram. Bull.*, 1979, **58**, pp. 1108–1110

7 PAEK, U. C., and RUNK, R. B.: 'Physical behavior of the neck-down region during furnace drawing of silica fibers', *J. Appl. Phys.*, 1978, **49**, pp. 4417–4422

8 PAEK, U. C., SCHROEDER, C. M., and KURKJIAN, C. R.: 'Determination of the viscosity of high silica glasses during fibre drawing', *Glass Technol.*, 1988, **29**, pp. 263–266

ROOM TEMPERATURE OPERATION OF MICRODISC LASERS WITH SUBMILLIAMP THRESHOLD CURRENT

A. F. J. Levi, R. E. Slusher, S. L. McCall, T. Tanbun-Ek, D. L. Coblentz and S. J. Pearton

Indexing terms: Lasers, Semiconductor lasers

Electrically pumped whispering-gallery mode microdisc lasers with singlemode operation and submilliamp threshold current at room temperature are demonstrated.

Purely electronic integrated circuits are made up of small, low power transistors connected by metal wires. In these circuits, electrical signals are generated and transported in the plane of the semiconductor substrate. Mass-production technology and high transistor packing density results in relatively low cost, highly functional circuits.

In contrast to electronics, optical devices, such as lasers, are expensive, large, and power hungry. It is, however, worthwhile investigating the possibility of using optical or optoelectronic structures to replace some of the functionality of electronic integrated circuits. In analogy with their successful counterpart, practical microphotonic circuits will be characterised by low cost, small size, low power consumption, and high optical confinement. In addition, light will be generated and guided in the plane of the semiconductor substrate.

In an attempt to meet some of the requirements outlined above we recently introduced the concept of a whispering-gallery mode microdisc laser [1]. The device consists of an InGaAs/InGaAsP multiple quantum well (MQW) structure formed into a 2–10 μm diameter disc approximately 0·1 μm thick. These microdiscs are supported on an InP pedestal. When optically pumped at liquid nitrogen temperature, lasing into the whispering-gallery resonant mode of the structure is observed with light emission in the plane of the disc and vertically as well owing to the presence of the pedestal.

We report our initial results in fabricating electrically pumped whispering-gallery mode microdisc lasers. We demonstrate singlemode operation and submilliamp threshold current at room temperature (T = 300 K).

The microdisc lasers used in our experiments were fabricated from InGaAsP crystals grown by organic vapour phase epitaxy to form the layer structure shown in Table 1. Photolithographic techniques were used to pattern metal contacts

Table 1 LAYER STRUCTURE

Material	Thickness	Impurity concentration
	μm	cm^{-3}
InGaAsP	0·3	$p = 3 \times 10^{18}$
InP	1·2	$p = 2 \times 10^{18}$
InGaAsP	0·11	0·0
InGaAs	0·01	0·0
InGaAsP	0·015	0·0
InGaAs	0·01	0·0
InGaAsP	0·015	0·0
InGaAs	0·01	0·0
InGaAsP	0·015	0·0
InGaAs	0·01	0·0
InGaAsP	0·11	0·0
InP	1·2	$n = 2 \times 10^{18}$
InP	Substrate	$n = 3 \times 10^{18}$

and etch cylinders of various diameters. An HCl solution was used to selectively etch away the InP above and below the quantum wells while leaving the InGaAsP MQW disc structure unetched. In Fig. 1 we show a scanning electron microscope image of a typical microdisc laser diode. Electrical contact to the top surface p-type InGaAs material is achieved using an approximately 4·5 μm diameter metal disc. The 5 μm diameter InGaAsP MQW laser disc in the Figure is supported above and below by an InP pedestal though which current j can flow.

In Fig. 2 we show room temperature pulsed current–light characteristics for a 9 μm diameter microdisc laser diode. Electrical pulses are 0·3 μs long with a 300 : 1 duty cycle. Light intensity L, emitted in the plane of the disc, is collected using a

lensed multimode fibre placed approximately 60 μm from the device. The kink in the $j - L$ characteristic shown in Fig. 2 corresponds to a laser threshold j_{th} of slightly less than 1 mA.

Fig. 1 *Scanning electron micrograph of laser diode structure*

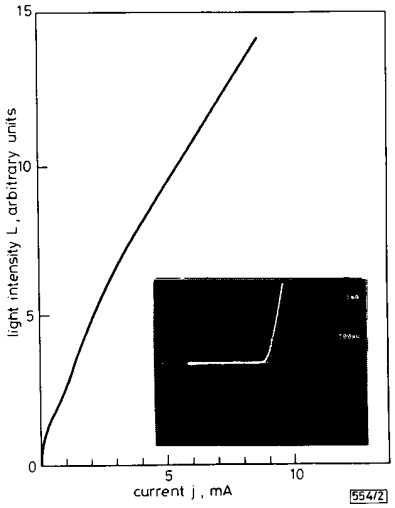

Fig. 2 *Light output L as function of current j*

Threshold current is $j_{th} = 0{\cdot}95$ mA
Measurements were performed at room temperature ($T = 300$ K) using 0·3 μs current pulses with 300 : 1 duty cycle
Inset: current–voltage characteristic of laser diode; 1 mA flows through diode at 1 V forward bias; series resistance of diode $R_s = 100\,\Omega$

We attribute the curvature in above threshold light intensity to a combination of current induced heating and gain saturation. Current induced heating is important at the relatively high current drive of $j = 8$ mA where doubling the current pulse width causes L to decrease by almost 10%. In addition, heating during the electrical pulse causes the lasing emission wavelength λ_i to shift resulting in a broadened effective line width.

The inset of Fig. 2 shows the current–voltage characteristic of the microdisc laser diode. The diode turn-on voltage is ~0·8 V and 1 mA of current flows at 1·0 V forward bias. The diode has a series resistance of approximately $R_s = 100\,\Omega$. R_s may be substantially reduced by increasing the p-type impurity concentration in the 0·3 μm thick InGaAsP contact layer (see Table 1).

Figs. 3 and 4 shows the detected light output spectrum for two representative values of current drive. Fig. 3 is the spectrum just above laser threshold with $j = 1$ mA. The triangle in Fig. 3 marks the peak in lasing emission at $\lambda_1 = 1{\cdot}580\,\mu$m. Note that the laser intensity is 9 dB (i.e. a factor of ~8) above the spontaneous emission background. Other devices with the same disc diameter but with higher j_{th} emit radiation into two or three modes at wavelengths $\lambda_1 = 1{\cdot}580\,\mu$m, $\lambda_2 = 1{\cdot}562\,\mu$m,

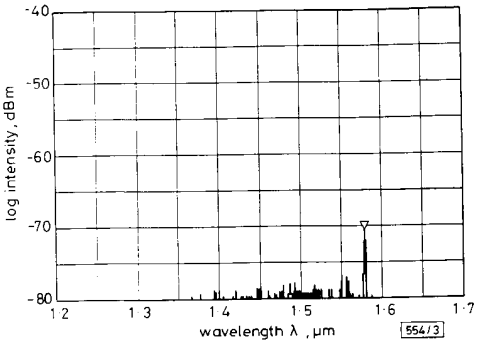

Fig. 3 *Measured room temperature spectrum for injection current of 1 mA*

▽ peak in lasing emission at $\lambda_1 = 1{\cdot}580\,\mu$m which is 9 dB above spontaneous emission background

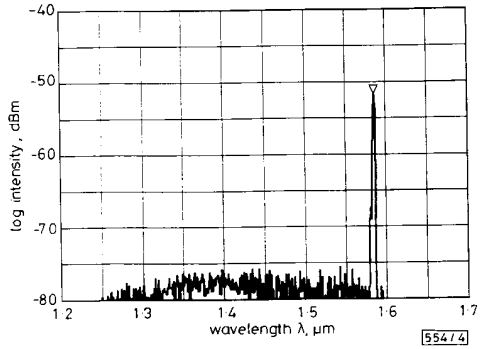

Fig. 4 *Measured room temperature spectrum for injection current of 8 mA*

▽ peak in lasing emission at $\lambda_1 = 1{\cdot}580\,\mu$m which is 26 dB above spontaneous emission background

and $\lambda_3 = 1{\cdot}549\,\mu$m. The spacings between modes are in the range expected for a disc resonator of diameter 9 μm [1]. Fig. 4 is the spectrum for $j = 8$ mA. Again, the triangle marks the peak in lasing emission at $\lambda_1 = 1{\cdot}580\,\mu$m. This time the peak intensity in the lasing line is 26 dB (i.e. a factor of ~400) above the spontaneous emission background. Note that the spontaneous emission background for $j = 8$ mA is greater than for $j = 1$ mA. This we tentatively ascribe to gain saturation and the associated weak pinning of the above threshold current carrier density.

In summary, we have demonstrated whispering-gallery mode microdisc lasers with singlemode operation and submilliamp threshold current at room temperature. Future publications will address issues related to the physics of device operation. For example, it is possible to decrease laser threshold current by reducing the electrically pumped volume (i.e. diameter) of the disc. However, when the diameter becomes comparable to the wavelength of light in the disc resonator other effects, such as enhanced coupling of spontaneous emission into the lasing mode, become important. This not only influences laser threshold current but also influences the temperature dependence of laser threshold current. We will also report on directional light coupling and guiding, high speed performance, and the functionality of microphotonic circuits.

Acknowledgment: We thank R. A. Keane for providing scanning electron microscope images.

30th March 1992

A. F. J. Levi, R. E. Slusher, S. L. McCall, T. Tanbun-Ek, D. L. Coblentz and S. J. Pearton (*AT&T Bell Laboratories, Murray Hill, New Jersey 07974, USA*)

References

1 MCCALL, S. L., LEVI, A. F. J., SLUSHER, R. E., PEARTON, S. J., and LOGAN, R. A.: 'Whispering-gallery mode microdisk lasers', *Appl. Phys. Lett.*, 1992, **60**, pp. 289–291

DISTORTION OF ANALOGUE INTENSITY MODULATED SIGNALS IN SEMICONDUCTOR OPTICAL AMPLIFIERS

A. N. Coles, J. A. Constable, I. H. White and D. G. Cunningham

Indexing terms: Optical amplifiers, Semiconductor devices, Optoelectronics, Harmonic distortion

Distortion of analogue intensity modulated signals amplified by near travelling wave semiconductor optical amplifiers, which is observed even for input optical powers significantly lower than saturation, is shown to be strongly influenced by residual facet reflectivity. Harmonic distortion levels have been observed to vary with wavelength by more than 12 dB.

Introduction: Semiconductor optical amplifiers have been shown to improve the performance of both digital [1] and analogue [2] optical communication systems. However, amplifier nonlinearities may result in crosstalk in intensity modulated wavelength division multiplexed systems [3] and pattern distortion in single channel digital intensity modulated systems [4]. In single channel analogue intensity modulated applications such as subcarrier multiplexed video distribution [2] and lightwave instrumentation, where system linearity is critical, amplifier nonlinearities generate harmonic distortion [5] and phase shifts. These nonlinearities arise from gain compression caused by depletion of the carrier density, and changes in the transmission of a near travelling wave amplifier cavity owing to the associated change in refractive index. Although studies of crosstalk have indicated a strong dependence on Fabry–Perot resonance, previous models of distortion in single channel systems have assumed an ideal travelling wave amplifier [6]. This Letter therefore reports an experimental and theoretical study of amplitude and phase distortion of a single analogue intensity modulated signal propagating through a semiconductor optical amplifier with Fabry–Perot resonance effects.

Experiment: An isolated distributed feedback laser (Toshiba TOLD 335S) at a wavelength of ~1311 nm is used as a source for experimental measurements. This is intensity modulated by an HP83421A $LiNbO_3$ Mach–Zehnder modulator. After minimising the harmonic distortion present on the electrical drive to the modulator and carefully adjusting the DC bias point to phase quadrature, the second harmonic distortion of the intensity modulation at the amplifier input is >30 dB (optical) below the fundamental, at a modulation index of 70%. A commercially available packaged semiconductor optical amplifier is used with peak material gain at 1302 nm and a 3 dB gain bandwidth of ~27 nm for a bias current of 50 mA. At this bias the peak fibre-to-fibre gain at the source wavelength is 5·6 dB, the depth of the gain ripple being 3·5 dB and the 3 dB saturation input power −7·5 dBm. Harmonic distortion of the intensity modulation at the amplifier output is measured using an HP71400A lightwave signal analyser, and the phase of the detected intensity modulation is monitored with a quadrature detector. By temperature tuning the laser wavelength it is possible to make measurements across one mode of the amplifier Fabry–Perot resonance.

The ratio of the fundamental to the second harmonic distortion of the intensity modulation at the amplifier output, and the phase of the fundamental relative to that at low input power, are plotted in Fig. 1 against power in the amplifier input fibre, for an input signal sinusoidally intensity modulated at 120 MHz. Results are plotted for four values of source wavelength corresponding to the peak, trough, rising edge and falling edge of the unsaturated amplifier Fabry–Perot resonance. When the source wavelength is tuned to the peak of the

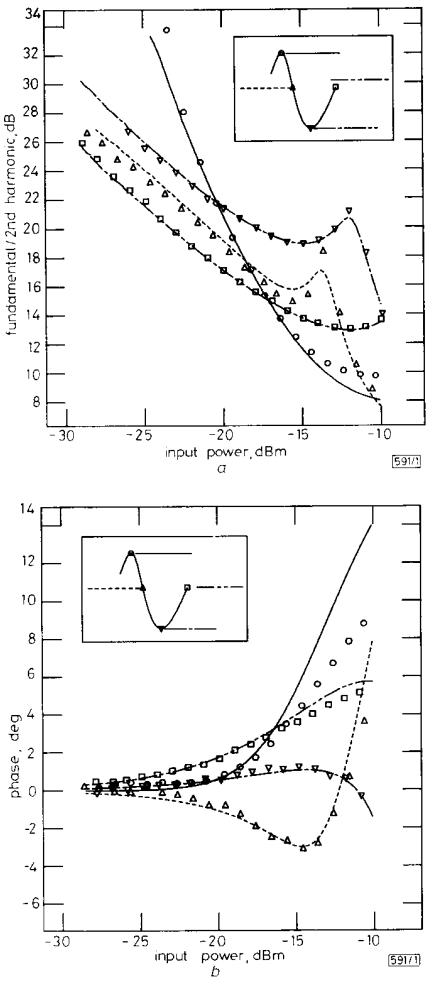

Fig. 1 *Experimental and theoretical plots of ratio of fundamental to second harmonic distortion and normalised phase of intensity modulation at amplifier output, against input power*

Inset: Signal wavelength (relative to unsaturated amplifier gain ripple)
Markers: experimental
——— theoretical
a Ratio of fundamental to second harmonic distortion
b Normalised phase

resonance, the ratio of fundamental to second harmonic falls from 28 dB (optical) at an input power 15 dB below saturation to 15·3 dB (optical) for an input power 10 dB below saturation. This ratio is also observed to peak sharply for certain combinations of input power and wavelength, and there are combinations at which the relative phase crosses zero. Experimental results for 1 GHz modulation frequency display similar trends, but the ratio of fundamental to second harmonic is improved by ~5 dB as the optically induced gain modulation response becomes limited by carrier lifetime.

The large variation in distortion seen in Fig. 1 as the source wavelength changes is better illustrated in Fig. 2, where fibre-to-fibre gain and the ratio of the fundamental to the second harmonic are plotted against source wavelength for −14 dBm input power. The distortion clearly depends significantly on the source wavelength detuning from the peak of the Fabry–Perot resonance. Two distinct wavelengths exist within one